A Catalogue of X-ray BL Lacs: Statistics Applied to the Study of X-ray Spectra

Rouco A., de la Calle I. & Racero E.

XMM-Newton SOC, European Space Astronomy Centre (ESAC), Madrid, Spain

An XMM-Newton Catalogue of BL Lac X-ray properties is presented based on the cross-correlation with the 1374 BL Lac objects listed in the 13th edition of the Véron-Cetty & Véron Catalogue. X-ray counterparts were searched for in the field of view of around 10000 XMM-Newton pointed observations that were public before May 2013. The cross-correlation yielded a total of 373 XMM-Newton observations which correspond to 106 different potential sources. Data from the three European Photon Imaging Cameras (EPIC) and Optical Monitor (OM) were homogeneously analyzed using the latest XMM-Newton SAS software. Phenomenological BL Lac emission models have been fitted systematically to all the X-ray spectra in order to characterize the X-ray properties of the sample.

We present the results of a study that investigates the use of different statistical methods for fitting X-ray spectra in the .0.2-10 keV energy band. With the fitting statistics defined, we compare the results of using two phenomenological models to characterize the X-ray emission, powerlaw vs log-parabolic, and look into the implications of using one versus the other in terms of model parameters.

INTRODUCTION

According to the unified scheme of active galactic nuclei (AGNs), a Blazar is considered to be any radio-loud AGN that displays highly variable, beamed, non-thermal emission covering a broad range from radio to γ-ray energies. The observed rapid variability and radio properties of these objects imply that they have relativistic jets whose axes make small angles with respect to the line of sight. Low-luminosity BL Lacs (High-energy peaked BL Lacs, or HBLs) present the first peak of their SED at UV-soft/X-ray band with the second one between the GeV and the TeV band (Padovani & Giommi 1995), while their higher luminosity counterparts present the first peak around IR/Optical energies (Low-energy peaked BL Lacs, or LBLs).

In general, Blazar emission is dominated by a broad, featureless continuum, believed to originate in the relativistic jet. Observationally, the SED of Blazars, in a $\nu F \nu$ representation, shows two broad distinctive peaks (Giommi & Padovani 1994). The first hump, peaking anywhere in the IR-soft X-ray range, is due to synchrotron emission, while the origin of higher energy one (usually at γ-ray frequencies) is still to be defined between processes of leptonic (Ghisellini 1999, Sikora 2001) or hadronic (Mücke 2003) nature.

The purpose of the present investigation is to contribute to the study of BL Lacs spectral characterization by extracting all the public available information on the X-ray (band pass 0.2-10 keV). We have only focused on the EPIC pn camera data and try to establish the best fit model for the sample in the catalogue, although all the information for the rest of the models will be available.

DATA SAMPLE

The sample used here is the result of the cross-correlation of the BL Lac sub-sample given in the Véron-Cetty & Véron Catalogue (2010, VC&C10) with all public observations available in the XMM-Newton archive up to May 2013. This BL Lac sub-sample consists of 1374 confirmed, probable or possible BL Lacs with or without a measured redshift. The initial cross-correlation is done by requesting that the VC&C10 sources fall inside any given XMM-Newton field of view. This match, yielded a total of 373 XMM-Newton observations corresponding to a potential 106 different sources.

After the screening process, 356 good observations remain. The discarded observations include: 11 where the source is outside the field FoV, and 6 bad observations. In 254 observations 90 different sources are detected and positively identified with the radio source, while in 102 observations no X-ray counterpart is detected and upper limits to the flux are derived for 14 different sources.

39/90 of the detected sources in our sample correspond to XMM-Newton targets.

51/90 sources are serendipitous.

71/104 of the sources have measured redshift, with an average of 0.38 and a maximun and minimun values of 5.03 and 0.029 respectively (Fig.1).

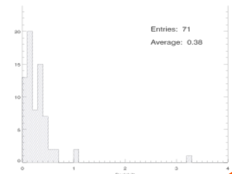

FIG. 1 Redshift distribution

STATISTICS SELECTION

χ^2 statistics applied to the X-ray spectra requires the spectral channels to be binned to contain at least 25 counts in each bin to apply the Gaussian approximation. On the other hand, the Cash statistic can be applied regardless of the number of counts in each spectral bin. Last, we want to point out a bias introduced with the use of χ^2 when we have a finite number of observed counts, (Siemiginowska et al. (2011)), Fig.2. Simulations show that the model-variance χ^2 statistic underestimates the power-law index and the data-variance χ^2 statistic overestimates it with respect to the results from the C statistic. Conversely, the Cash statistic returns more reliable results (Nousek & Shue (1989); Humphrey et al. (2009)).

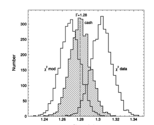

Fig.2 Distributions of a single power-law model photon index obtained by fitting simulated X-ray spectra with 60,000 counts and using the three different statistics: χ^2 with model variance, χ^2 with data variance and Cash statistics. Credits: Siemiginowska et al. (2011)

The Poisson distribution becomes Gaussian as the number of counts increases, the former is pretty close to the latter. To ensure Gaussian statistics we require a spectral binning such that a minimun number of 25 counts are present per channel and a minimun of 3 spectral channels so as to not to oversample the energy resolution. We produce ratio of data to best fit model files for each individual spectrum to create stacked spectra (averaged spectra of residuals).

3 options are available: χ^2 statistic model weighted (CHIMOD), χ^2 statistic standard (data) weighted (CHISTD) and C statistic standard weighted (CSTAT). In the 3 cases, the *goodness of fit* (GOF) has been calculated with the χ^2 test statistics.

500-20000 COUNTS (ungrouped)

PARAMETERS, sdev	Fit_cstat	Fit_chistd	Fit_chimod
Alpha	[illegible]	[illegible]	[illegible]
log(Soft Flux) (10^-11 erg/cm^2/s)	[illegible]	[illegible]	[illegible]
log(Hard Flux) (10^-11 erg/cm^2/s)	[illegible]	[illegible]	[illegible]
nH (10^22 g/cm^2)	[illegible]	[illegible]	[illegible]
GOF	[illegible]	[illegible]	[illegible]
N. Good ObsIDs	[illegible]	[illegible]	[illegible]
N. Bad ObsIDs	[illegible]	[illegible]	[illegible]

20000-70000 COUNTS (ungrouped)

PARAMETERS, sdev	Fit_cstat	Fit_chistd	Fit_chimod
Alpha	[illegible]	[illegible]	[illegible]
log(Soft Flux) (10^-11 erg/cm^2/s)	[illegible]	[illegible]	[illegible]
log(Hard Flux) (10^-11 erg/cm^2/s)	[illegible]	[illegible]	[illegible]
nH (10^22 g/cm^2)	[illegible]	[illegible]	[illegible]
GOF	[illegible]	[illegible]	[illegible]
N. Good ObsIDs	[illegible]	[illegible]	[illegible]
N. Bad ObsIDs	[illegible]	[illegible]	[illegible]

MORE THAN 70000 COUNTS (ungrouped)

PARAMETERS, sdev	Fit_cstat	Fit_chistd	Fit_chimod
Alpha	[illegible]	[illegible]	[illegible]
log(Soft Flux) (10^-11 erg/cm^2/s)	[illegible]	[illegible]	[illegible]
log(Hard Flux) (10^-11 erg/cm^2/s)	[illegible]	[illegible]	[illegible]
nH (10^22 g/cm^2)	[illegible]	[illegible]	[illegible]
GOF	[illegible]	[illegible]	[illegible]
N. Good ObsIDs	[illegible]	[illegible]	[illegible]
N. Bad ObsIDs	[illegible]	[illegible]	[illegible]

500-20000 COUNTS — SUMMARY OF PARAMETERS

PARAMETERS, sdev	Fit_cstat	Fit_chistd	Fit_chimod
Alpha	2.28+/- 0.12, 0.39	2.30+/- 0.12, 0.40	2.27+/- 0.12, 0.39
log(Soft Flux) (10^-11 erg/cm^2/s)	0.87+/- 0.16, 0.55	0.88+/- 0.17, 0.55	0.87+/- 0.16, 0.55
log(Hard Flux) (10^-11 erg/cm^2/s)	0.91+/- 0.15, 0.49	0.93+/- 0.15, 0.49	0.90+/- 0.15, 0.49
nH (10^22 g/cm^2)	0.21+/- 0.14, 0.47	0.22+/- 0.15, 0.50	0.21+/- 0.15, 0.49
GOF	1.068+/- 0.060, 0.199	1.047+/- 0.058, 0.193	1.072+/- 0.061, 0.202
N. Good ObsIDs	11	11	11
N. Bad ObsIDs	0	0	0

20000-70000 COUNTS — SUMMARY OF PARAMETERS

PARAMETERS, sdev	Fit_cstat	Fit_chistd	Fit_chimod
Alpha	2.33+/- 0.10, 0.35	2.35+/- 0.10, 0.36	2.368+/-0.098, 0.326
log(Soft Flux) (10^-11 erg/cm^2/s)	0.08+/- 0.13, 0.45	0.08+/- 0.13, 0.45	0.05+/- 0.14, 0.46
log(Hard Flux) (10^-11 erg/cm^2/s)	0.21+/- 0.17, 0.57	0.22+/- 0.17, 0.57	0.20+/- 0.18, 0.60
nH (10^22 g/cm^2)	0.030+/- 0.010, 0.036	0.033+/- 0.011, 0.038	0.031+/- 0.011, 0.036
GOF	1.328+/- 0.062, 0.215	1.312+/- 0.062, 0.214	1.292+/- 0.041, 0.137
N. Good ObsIDs	12	12	11
N. Bad ObsIDs	0	0	1

MORE THAN 70000 COUNTS — SUMMARY OF PARAMETERS

PARAMETERS, sdev	Fit_cstat	Fit_chistd	Fit_chimod
Alpha	2.506+/-0.061, 0.212	2.511+/-0.061, 0.212	2.504+/-0.061, 0.213
log(Soft Flux) (10^-11 erg/cm^2/s)	1.54+/- 0.12, 0.42	1.54+/- 0.12, 0.42	1.54+/- 0.12, 0.42
log(Hard Flux) (10^-11 erg/cm^2/s)	1.88+/- 0.12, 0.42	1.89+/- 0.12, 0.42	1.88+/- 0.12, 0.42
nH (10^22 g/cm^2)	0.0220+/- 0.0041, 0.0141	0.0226+/- 0.0041, 0.0142	0.0217+/- 0.0040, 0.0140
GOF	1.483+/- 0.094, 0.326	1.442+/- 0.087, 0.303	1.442+/- 0.087, 0.303
N. Good ObsIDs	12	12	12
N. Bad ObsIDs	1	1	1

Table 1. Summary of average parameters for the ungrouped (left) and grouped (right) spectra when using different statistics on the 3 counts ranges.

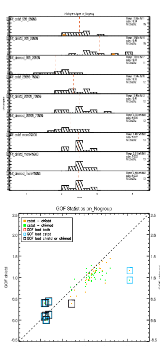

Fig.3 Top: Histogram displaying distribution of alpha index parameter and comparing statistics for ungrouped spectra for different count rates. Bottom: GOF plot comparing statistics for ungrouped spectra. Squares show observations with bad GOF (GOF≤0.5 or GOF≥2) .

- The GOF is CSTAT where the averaged GOF is practically 1 (Table 1), true at least for the lower counts range.
- For the intermediate and high counts ranges, all statistics behave in a similar maner, the averaged model parameters are within errors.
- The plot (bottom Fig.3) shows that most of the CHISTD and CHIMOD GOF are sistematically lower than CSTAT GOF. This is supported by the stacked spectra of the residuals, Fig.4, where it is clear that CHISTD and CHIMOD fits are on average poor for the low counts range.
- Similar results as those found by Siemiginowska et al. (2011), top Fig.3
- Grouping our data makes all the results very estable.
- We decided to use C statistic on grouped spectra: C statistic works on all counts regimes, but XSPEC does not handle properly bins with 0 counts or deals properly with the background counts.

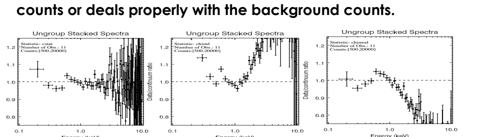

Fig. 4 Stacked spectra plots of residuals for ungroup spectra for low count rate, model PowerLaw2ABS. First CSTAT, second CHISTD and third CHIMOD.

MODEL SELECTION

2 models have been fitted to each EPIC spectrum:

1. A Single Power: $$\frac{dN}{dE} = \kappa e^{-\sigma(E) N_{H,Gal}} e^{-\sigma(E) N_{H,int}(1+z)} E^{-\alpha}$$

2. A Logarithmic Parabola: $$\frac{dN}{dE} = \kappa e^{-\sigma(E) N_{H,Gal}} e^{-\sigma(E) N_{H,int}(1+z)} E^{(-\alpha-\beta Log(E))}$$

In each case, we performed fits with three different treatments of the absorption: *a*) with the absorption component fixed to the galactic column density $N_{H,Gal}$ (with $N_{H,int}$ = 0) taken from *Leiden/Argentine/Bonn (LAB) Survey of Galactic HI*, *b*) with the galactic column density let to vary free (with $N_{H,int}$ = 0) and *c*) with two contributions $N_{H,Gal}$ fixed to the galactic column density and *NH,int* let to vary free but always higher than *NH,Gal*. *NH,int* accounts for any internal source absorption, and is hence a function of the redshift.

SUMMARY OF PARAMETERS

PARAMETERS, sdev	PowerLaw2ABS	PowerLawFree	PowerLawFixed
Alpha	2.408+/- 0.029, 0.353	2.398+/- 0.029, 0.354	2.267+/- 0.033, 0.402
log(Soft Flux) (10^-11 erg/cm^2/s)	0.285+/- 0.070, 0.851	0.257+/- 0.070, 0.851	0.368+/- 0.079, 0.811
log(Hard Flux) (10^-11 erg/cm^2/s)	0.539+/- 0.065, 0.789	0.517+/- 0.065, 0.789	0.651+/- 0.074, 0.762
nH (10^22 g/cm^2)	0.0518+/- 0.0127, 0.1534	0.0732+/- 0.0096, 0.1176	0.0350+/- 0.0035, 0.036
GOF	1.168+/- 0.021, 0.250	1.160+/- 0.021, 0.253	1.249+/- 0.027, 0.281
N. Good ObsIDs	146	150	105
N. Bad ObsIDs	51	47	92
Statistics Summatory	123444.	119702.	229977.

SUMMARY OF PARAMETERS

PARAMETERS, sdev	LogPar2ABS	LogParFree	LogParFixed
Alpha	2.530+/- 0.045, 0.565	2.471+/- 0.047, 0.600	2.092+/- 0.052, 0.660
Beta	0.081+/- 0.024, 0.308	0.045+/- 0.027, 0.347	0.146+/- 0.026, 0.330
log(Soft Flux) (10^-11 erg/cm^2/s)	0.200+/- 0.070, 0.891	0.184+/- 0.070, 0.891	0.145+/- 0.071, 0.879
log(Hard Flux) (10^-11 erg/cm^2/s)	0.451+/- 0.064, 0.812	0.442+/- 0.064, 0.812	0.450+/- 0.067, 0.826
nH (10^22 g/cm^2)	0.0517+/- 0.0093, 0.1184	0.0749+/- 0.0091, 0.1154	0.0369+/- 0.0039, 0.048
GOF	1.108+/- 0.016, 0.209	1.092+/- 0.016, 0.198	1.139+/- 0.019, 0.228
N. Good ObsIDs	161	160	152
N. Bad ObsIDs	36	37	45
Statistics Summatory	87019.3	75610.2	94003.7

Table 2. Summary of average parameters for the grouped spectra when using Power law (left) and Logarithmic parabola (right) model and three flavours of the absorption component.

- Regarding the GOF, we see that both Powerlaw and Logpar models with nHFree and nH2ABS provide on average better fits than with nHFixed. It is supported by their fit statistics summatories, whose values is considerably lower (better fit).
- The study of the stacked spectra residuals confirms this (Fig.6).
- We point out the following consideration when comparing nHFree vs nH2ABS: The free component of the model with two absorption components is limited to never be lower than nHGal. This can introduce a bias in this extra component towards higher nH values, which is translated into a bias in the Power law index.
- It is clear that, in the case PowerLaw2ABS-PowerLawFixed, the values of the alpha parameter are truncated (Fig.5 up). It means that the PowerLaw2ABS alphas are sistematically higher. The reason for this behaviour is that the nH free component of this model is limited to the galactic value, therefore if XSPEC is not able to make that parameter lower, then it compensates by making the alpha value higher in the fitting process.

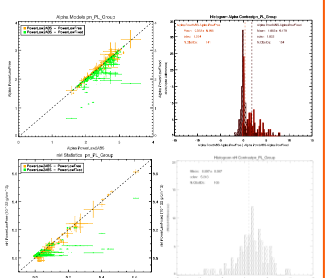

Fig.5 Up left: Plot comparing alpha (photon index) for PowerLaw2ABS-PowerLawFree (orange) and PowerLaw2ABS-PowerLawFixed (green). Up right: Histogram displaying differences distributions for alpha parameter (weighted by their errors). Orange line corresponds to alphaPow2ABS-alphaPowFree and black line to alphaPow2ABS-alphaPowFixed. Bottom Left: Plot comparing nH for PowerLaw2ABS-PowerLawFree (orange) and PowerLaw2ABS-PowerLawFixed (green). Bottom Right: Histogram displaying differences distributions for nH parameter (weighted by their errors), nHPowFree-nHPowFixed.

- Fig.5 bottom shows the comparision of nH as obtained by the 3 different flavours of nH. Comparing the values of nH obtained for the PowerLawFree and those used in the PowerLawFixed, we could test if we are introducing a bias by limiting to >nHGal the free component. There are several cases where the nH value should be < galactic value.
- The inclusion of beta (curvature) in Logarithmic parabola model, introduces complexity that it is not significantly required by the data.

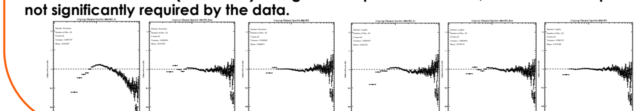

Fig.6 Stacked spectra of residuals for Power law model (left) and Loragarithmic parabola model (left).

SUMMARY AND FUTURE WORK

- An XMM-Newton catalogue of BL Lacs X-ray properties has been produced by searching the XSA archive for X-ray counterparts of the 1374 BL Lacs listed in VC&V10 Catalogue.
- A study to investigate the use of different statistical methods for fitting the X-ray spectra shows that C statistic is the best option to fit all the catalogue X-ray espectra. It is the most reliable option even in the low count rate range.
- The selection of the best fit model is based on the averaged goodness of fit, the stacked spectra residuals and averaged parameter properties. For that reason, we have choosen the Power law model with a free component of nH to fit the spectra of the sample.
- The same study developed in this work should be done for the data combined from the three EPIC cameras (pn, MOS1 and MOS2). Using the 3 cameras combined would increase our statistics.
- To develop the same templates as in XSPEC for ISIS to work with ungrouped spectra and run it in a systematic way over the whole sample.
- The information in the catalogue, together with information at other wavelengths, will allow us to identify Blazar candidates at TeV energies .

References:

Ghisellini, G., 1999, Astropart. Phys., 11;Mücke, A., et al., 2003,Astropart. Phys., 18, 593
Humphrey P., Liu W., Buote D., 2009, ApJ, 693, 822;Nousek J., Shue D., 1989, ApJ, 342, 1207
Sikora, M., & Madejski, G., 2001,AIP Conference Pro.;Padovani, P., & Giommi, P., 1995; ApJ, 444, 567
Véron-Cetty, M. P., & Véron, P., 2010,A&A, 518, A10;Siemiginowska A., Arnaud K., Smith R., 2011, Handbook of X-ray

CONTACT: arouco@sciops.esa.int

We acknowledge support from the Faculty of the European Space Astronomy Centre (ESAC)